Theoretical analysis of the bias-voltage dependence of the apparent barrier height

H. Totsuka,[1,3] Y. Gohda,[2,3] S. Furuya,[2,3] and S. Watanabe[2,3]

[1]*Department of Physics, College of Science and Technology, Nihon University, 1-8-14 Kanda-Surugadai, Chiyoda-ku, Tokyo 101-8308, Japan*

[2]*Department of Materials Science, The University of Tokyo, 7-3-1 Hongo, Bunkyo-ku, Tokyo 113-8657, Japan*

[3]*CREST, Japan Science and Technology Corporation, 4-1-8 Honcho, Kawaguchi-shi, Saitama 332-0012, Japan*

We have analyzed the bias voltage dependence of the apparent barrier height (ABH), using a self-consistent calculation within the density functional theory. We have found that the ABH shows the bias polarity dependence in both of the two Al(100) surfaces, the one without reconstruction and the one containing the vacancy cluster in the layer next to the surface. We have also found that the surfaces have opposite bias polarity dependences of the ABH. These results cannot be understood in the light of the formation of the surface dipole layer, but can be understood from two factors: the reduction in the effective potential and the change in the surface electron states by the applied bias voltage.

I. INTRODUCTION

Apparent barrier height (ABH), which is a barrier height for tunneling electrons estimated from the change of tunneling current with the variation of tip-sample separation in scanning tunneling microscopy (STM), provides us with rich information on the properties of materials. The ABH was measured by Binnig and Rohrer[1] and they showed the possibility that the ABH profiles eventually have a resolution similar to that of the STM topography. Wiesendanger *et al.*[2] measured the ABH on surfaces of several systems such as graphite and metallic glasses. They showed that the ABH measurements provide useful information about chemical inhomogeneities and crystallographic anisotropies. Since their measurements, the ABH images have been obtained for various surfaces.[3–7] The ABH measurements not only revealed the size of defects on Si(001) (Ref. 4) but also distinguished between vacancies and interstitial defects on graphite surfaces.[5] Further, the ABH was used to evaluate the capacitance of a nanometer-thickness organic overlayer.[8] In addition, the tip-sample separation dependence of the ABH was studied for Au(100) surface.[9]

Recently, the bias voltage dependence of the ABH has attracted attention,[10–13] in expectation to get information on, for example, surface charge distribution. For example, it was used to study the qualitative difference of band-bending effects between passivated and unpassivated semiconductor surfaces.[10] The stability of Pb islands on Si(111) was also studied.[11] In some such measurements, special attention was paid to the bias polarity dependence: the ABH on the reconstructed Au(111) surface was found to show a bias polarity dependence, and this dependence was speculated to come from the surface dipole layer originating from the reconstruction.[12,13]

In the measurements as above, the ABH ϕ_{app} has been estimated using the formula

$$\phi_{app}(\text{eV}) = 0.952 \left(\frac{d \ln I_t}{ds(\text{Å})} \right)^2, \qquad (1)$$

where I_t and s are the tunneling current and the tip-sample separation, respectively. This equation is derived by the

Wentzel-Kramers-Brillouin method on the basis of one-dimensional square potential and constant bias voltage. Since this potential simplifies realistic tip and sample structures too much and the bias voltage dependence is not considered, it is not easy to interpret the ABH evaluated by Eq. (1). Theoretically, Lang[14] analyzed the ABH using calculation of the tunneling current within the local density approximation, and pointed out that it can be smaller than the actual work function of the sample for separations commonly encountered experimentally. Hirose and Tsukada[15] also analyzed the barrier height, considering slightly more realistic sample structures, and showed that the microscopic shape of the tunneling barrier strongly depends on the tip-surface distance and the bias voltage in cases where the tip and sample are nearly in contact. Our previous study showed that the ABH on the site above a vacancy cluster is smaller than the one on the clean Al(100) surface because of the difference of the decay rate of electron density around the sample surface.[16] However, the bias voltage dependence of the ABH, which is usually the more important information obtained from measurements, has not been analyzed at all.

In the present paper, we report the results of our theoretical analysis of the effects of the bias voltage on the ABH, employing the method to calculate electronic states under an applied bias voltage self-consistently within the density functional theory[17,18] and taking Al surfaces as an example. We have found that even the ABH on the clean Al(100) surface shows a bias polarity dependence, and that the bias dependence of the ABH on the site above a vacancy cluster is opposite to that on the clean surface. Furthermore, we show that the difference between the two cases cannot be attributed to the formation of an additional surface dipole layer.

II. METHOD

In the present analysis, one-electron effective potential and tunneling currents are calculated by the method in which the Kohn-Sham equation[19,20] is solved for a given energy and a given surface-parallel wave vector including scattering

states explicitly.[17,18] The single-particle wave function and effective potential are expanded in terms of plane waves in directions parallel to the surface. Cutoff energy for this expansion is set to be 3.88 Ry. For the exchange-correlation potential, we adopt the Ceperley-Alder form within the local density approximation.[21] For the ionic potential of Al, we adopt a pseudopotential proposed by Chelikowsky *et al.*[22] Hartree potential is calculated together with external electrostatic potential by solving the Poisson equation.

The bias voltage in this method is defined according to Büttiker *et al.*,[23] i.e., Fermi levels of respective electrodes are adjusted to keep charge neutrality in electrodes during calculations,[24] while the bias voltage is defined as the difference between Fermi levels of the electrodes before the adjustment. Since electrodes of a sample and a tip are the same metal in the present study, it is obvious that the applied bias voltage corresponds to the difference in the Fermi levels of deep insides of the electrodes. On the other hand, the applied voltage does not necessarily correspond to the difference in the Fermi levels of subsurface regions of the electrodes, because partial transmission of electron waves from electrode A to electrode B causes deficit (excess) of electrons in electrode $A(B)$ and charge unbalance accompanied by this should be recovered by adjusting the Fermi levels. Because these shifts of the Fermi levels in the subsurface regions do not affect the Fermi levels of deep insides owing to relaxation processes due to inelastic scattering, it is appropriate to define the bias voltage as the difference of Fermi level before adjusting the Fermi levels.

III. MODELS

As a model for STM, an STM tip and a sample surface are represented by an Al atom attached to a semi-infinite jellium electrode and two layers of Al(100) attached to another semi-infinite jellium electrode, respectively.[16] For sample surfaces, in addition to the model above, we also examine another one where four Al atoms are missing in the layer next to the surface.[16] This model structure is unstable and thus unrealistic, in the sense that the structure relaxation, which must be considerable in the model, is neglected. Because of this, direct comparison between our results and experiments may be difficult. However, our model has no serious weak points to examine the effects of electronic states on the ABH. Further, the effects of the electronic states are not specific to our model. For example, the most crucial feature of our model, the existence of localized states, is expected to appear in various other systems. Therefore, we can say that our work provides information useful for the studies of the ABH in general. The tip-sample separation is defined as the distance between the tip atom and the surface Al layer in the sample, the value of which is taken to be 5.8 Å in all the calculations. The Wigner-Seitz radius of the two jellium electrodes is taken to be 2 atomic units, which is nearly the same as that of bulk Al. The area of the unit cell in the directions parallel to the surface is set to be 8.6×8.6 (Å)^2. Hereafter we call the first and second models nondefective and defective samples, respectively.

We evaluate the barrier height for tunneling electrons from the calculated results by two methods. In the first one,
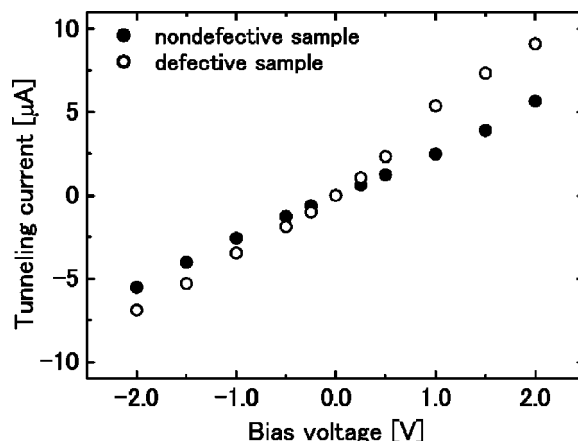

FIG. 1. Calculated tunneling currents as a function of the bias voltage. Open and solid circles denote the currents for the nondefective and defective samples, respectively.

Eq. (1) is used, approximating the derivative by the difference

$$\phi_{\mathrm{app}}(d) = 0.952 \left(\frac{1}{\Delta d} \ln \frac{I_t(d + 0.5\Delta d)}{I_t(d - 0.5\Delta d)} \right)^2, \qquad (2)$$

where d denotes the tip-sample separation. The tunneling current I_t is defined as the integration of tunneling current density within the unit cell. We set Δd to be 0.2 Å according to a typical experimental condition.[3,4] In the second, the barrier height is defined as a maximum value of the calculated potential on a straight line perpendicular to the surfaces, which penetrates both the atom above the vacancy cluster and the tip atom.[14] Hereafter, we call the barrier heights evaluated using the first and second methods ABH and maximum barrier height (MBH), respectively.

IV. RESULTS

Figure 1 shows calculated tunneling current (I)-voltage (V) characteristics of the nondefective and defective samples. From Fig. 1, we can see that the I-V curve of the nondefective sample is almost linear and symmetric on the bias polarity. On the other hand, for the defective sample, the I-V curve is not linear, and asymmetric on the bias polarity. This bias polarity dependence for the defective sample can be understood from the existence of localized states in front of an atom above a vacancy cluster at $E_F^S + 2$ V, where E_F^S denotes the Fermi level of the surface. It should be noted that these localized states come to appear notably with an increase in the bias voltage.

The calculated MBH and ABH of the nondefective and the defective samples are presented in Fig. 2. The fact seen in Figs. 2(a) and 2(b) that the value of the ABH is larger than that of the MBH is explained by the lateral confinement of tunneling electrons.[14,15] The ABH difference between the nondefective and the defective samples can be attributed to the difference of the decay constant.[16] As for the bias voltage dependence of the ABH, there are three notable features. First, even the nondefective sample shows the bias polarity
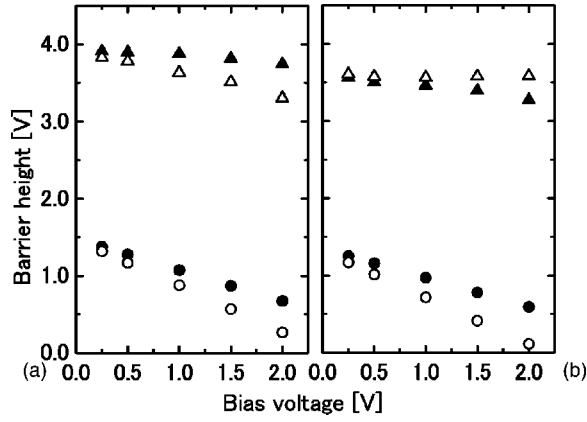
FIG. 2. Maximum barrier height (MBH) and apparent barrier height (ABH) of the (a) nondefective and (b) defective samples. Open and solid circles denote the MBH for the positive and negative bias voltages, respectively. Open and solid squares denote the ABH for the positive and negative bias voltages, respectively. Straight lines are guides for the eyes.

dependence. As seen in Fig. 2(a), the ABH at a negative bias voltage is always larger than that at the corresponding positive voltage. We can also see that the difference of the ABH by bias polarity is small at low bias voltage and becomes larger with an increase in bias voltage. This feature is consistent with the experimental results by Yagyu and Yoshitake.[13] It should be noted that for this sample, the difference of the MBH by the bias polarity exhibits behavior similar to that of the ABH. Second, the defective sample shows the polarity dependence of the ABH opposite to the nondefective sample. This feature, that the ABH at a positive bias voltage is larger than that at the corresponding negative one, is consistent to the experimental results by Mizutani *et al.*[12] It is worth mentioning, on the other hand, that the difference of the MBH by the bias voltage exhibits behavior similar to that of the nondefective sample. Third, the ABH decreases monotonically in all the samples and polarities we studied except for the positive bias of the defective sample, where the ABH takes its minimum at about +1 V.

Traditionally, the formation of a surface dipole layer is considered a strong candidate, when trying to determine the origin of the above feature of the ABH.[8,12,25] However, we found that the bias voltage dependence of the ABH in our results cannot be understood from the surface dipole layer, as described below. In Figs. 3(a) and 3(b), we show calculated electron density on the line which is perpendicular to the surface and passes through the top atom of the tip at bias voltages of −2, 0, and +2 V, together with the differences of electron density at −2 and +2 V from that at 0 V. These figures reveal that the surface dipole layer forms in both cases of the nondefective and the defective samples, and its characteristics are similar in both cases. Further, we can see that the change of electron density distribution due to the applied bias voltage is almost the same in the two samples. Therefore, we can conclude that the formation of the surface dipole layer does not cause the bias voltage dependence of the ABH.[26]

To proceed with our discussion on the origin of the bias polarity dependence of the ABH, we emphasize that the difference of the ABH implies the different behavior of the decay of wave functions: The decay constant of the wave functions with total energy E is given in atomic units[27] as

$$\kappa^2 \propto V(z) - E_z(\mathbf{k}_\parallel), \quad E_z = E - \frac{k_\parallel^2}{2}, \quad (3)$$

where V and $\mathbf{k}_\parallel$ are the effective potential and a wave vector component parallel to the surface, respectively. Therefore, we analyzed the E_z distribution of electron density in the vacuum region. In this analysis, we define the vacuum region as the region where the effective potential is higher than the higher Fermi level of those of the two electrodes.

Figures 4(a) and 4(b) show calculated E_z distribution of electron density of the nondefective and defective samples at the bias voltages of −2 and +2 V, respectively. It is noted that the degree of wave functions spilled into the vacuum shown in Fig. 4 is not considered to depend on the unit cell size strongly, since the wave function spill from the place other than the tip apex is small because of the large potential
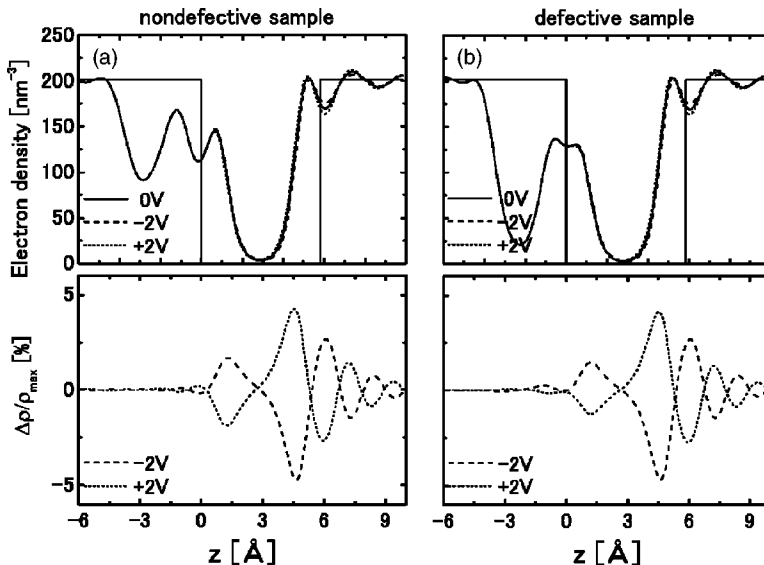

FIG. 3. Calculated electron density distribution and $\Delta\rho/\rho_{max}$ of the (a) nondefective and (b) defective samples at the bias voltages of −2, 0, and +2 V, respectively. Solid, long-dotted and dotted lines donote the electron density at the bias voltages of −2, 0, and +2 V, respectively. Here $\Delta\rho$ and ρ_{max} are defined as the difference of electron density at −2 and +2 V from that at 0 V and the maximum value of the electron density at 0 V, respectively.
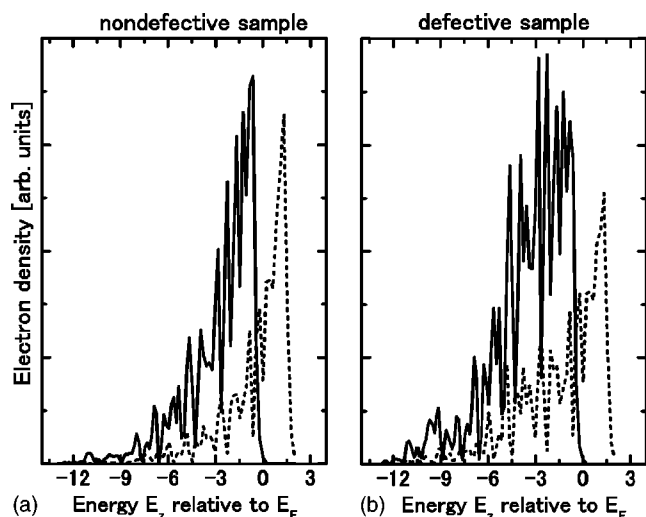
FIG. 4. Calculated electron density distribution of the (a) non-defective and (b) defective samples as a function of the kinetic energy perpendicular to the surface E_z. Solid and dotted lines denote the electron density at the bias voltages of -2 and $+2$ V, respectively.

barrier. In the case of the nondefective sample, the E_z distribution of the electron density changes little with the bias polarity, as can be seen in Fig. 4(a). On the other hand, the bias polarity dependence of the ABH is similar to that of the MBH. Therefore, the difference of the ABH can be attributed to the difference of the potential barrier height. The origin of the bias polarity of the MBH can be understood from the fact that at positive bias voltages, the potential decreases locally in front of the tip apex.[28] This local potential decrease is due to concentration of the induced electron density in front of the tip. On the contrary, in the case of negative bias voltage, the degree of the potential decrease is smaller because of flat geometry of the sample surface.

In the case of the defective sample, Fig. 2(b) shows that the ABH of positive bias increases in the bias voltage range of $+0.5$ V $\leq V_{bias} \leq +2$ V although the MBH decreases with the increase in the bias voltage. This is understood as follows. From Eq. (3), we can expect an increase in the decay rate, when the E_z distribution of electron density near the Fermi level decreases as the bias voltage increases. If this effect is larger than that of the effective potential reduction,

the ABH increases. In fact, from Fig. 4(b), it is seen that the electron density at a bias voltage of -2 V is larger than that at a bias voltage of $+2$ V in all energy ranges. We can say that this decrease in the electron density at a bias voltage of $+2$ V causes the increase in the ABH. The decrease in this electron density is understood from the existence of electronic states localized on the site above the vacancy cluster at a bias voltage of $+2$ V. Since the motion of the localized states is confined spatially to the direction parallel to the surface, this confinement causes a decrease in the energy available for motion along the direction perpendicular to the surface. Therefore, we can conclude that the increase in the ABH in positive bias is attributed to the decrease in the electron density due to the electronic states localized on the site above the vacancy cluster.

V. CONCLUSIONS

In conclusion, we analyzed the bias voltage dependence of the apparent barrier height (ABH), using self-consistent calculation within the density functional theory. We have found that the ABH shows the bias polarity dependence in both cases of the two Al(100) surfaces, the one without reconstruction and the one containing the vacancy cluster in the layer next to the surface. We have also found that the polarity dependence of the ABH is opposite in the two cases. These results cannot be understood in the light of the formation of the surface dipole layer, but can be understood from two factors: the reduction in the effective potential and the change in the surface electron states by the bias voltage. So far, we have not succeeded yet in establishing procedure to draw useful information from the observed bias-voltage dependence of the apparent barrier height. However, we can say that the effects of electronic states on them clarified in the present work should be important in interpreting the observed data. It is noted that to clarify the effects of other factors, such as structural relaxation due to the applied bias voltages and currents, remains a future problem.

[1] G. Binnig and H. Rohrer, Surf. Sci. **126**, 236 (1983).

[2] R. Wiesendanger, L. Eng, H. R. Hidber, P. Oelhafen, L. Rosenthaler, U. Staufer, and H. J. Güntherodt, Surf. Sci. **189/190**, 24 (1987).

[3] J. F. Jia, K. Inoue, Y. Hasegawa, W. S. Yang, and T. Sakurai, Phys. Rev. B **58**, 1193 (1998).

[4] R. J. Hamers and U. K. Kohler, J. Vac. Sci. Technol. A **7**, 2854 (1989).

[5] J. R. Hahn and H. Kang, Phys. Rev. B **60**, 6007 (1999).

[6] B. Marchon, P. Bernhardt, M. E. Bussell, G. A. Somorjai, M. Salmeron, and W. Siekhaus, Phys. Rev. Lett. **60**, 1166 (1987).

[7] J. S. Villarrubia and J. J. Boland, Phys. Rev. Lett. **63**, 306 (1989); M. Yoon, H. Mai, and R. F. Willis, Europhys. Lett. **54**, 626 (2001); J. Yoshikawa, S. Kurokawa, and A. Sakai, Appl. Surf. Sci. **169-170**, 202 (2001).

[8] J. K. Spong, Nature (London) **338**, 137 (1989); R. Akiyama, T. Matsumoto, and T. Kawai, Phys. Rev. B **62**, 2034 (2000).

[9] Y. Kuk and P. J. Silverman, J. Vac. Sci. Technol. A **8**, 289 (1990).

[10] M. Weimer, J. Kramar, and J. D. Baldeschwieler, Phys. Rev. B **39**, 5572 (1989); R. M. Silver, J. A. Dagate, and W. Tseng, J. Appl. Phys. **76**, 5122 (1994); S. Hearne and G. Hughes, Appl. Surf. Sci. **123/124**, 176 (1998).

[11] M. Hupalo and M. C. Tringides, Phys. Rev. B **65**, 115406 (2002).

[12] W. Mizutani, T. Ishida, N. Choi, T. Uchihahashi, and H. Tokumoto, Appl. Phys. A: Mater. Sci. Process. **72**, S181 (2001).

[13] S. Yagyu and M. Yoshitake, J. Vac. Sci. Technol. A **21**, 1294 (2003); S. Yagyu, Surf. Sci. **532-535**, 1136 (2003).

[14] N. D. Lang, Phys. Rev. B **37**, 10 395 (1988).

[15] K. Hirose and M. Tsukada, Phys. Rev. Lett. **73**, 150 (1994); Phys. Rev. B **51**, 5278 (1995).

[16] H. Totsuka, S. Furuya, Y. Gohda, and S. Watanabe, Jpn. J. Appl. Phys., Part 2 **41**, 1172 (2002).

[17] Y. Gohda, Y. Nakamura, K. Watanabe, and S. Watanabe, Phys. Rev. Lett. **85**, 1750 (2000).

[18] S. Furuya, Y. Gohda, N. Sasaki, and S. Watanabe, Jpn. J. Appl. Phys., Part 2 **41**, 989 (2002).

[19] P. Hohenberg and W. Kohn, Phys. Rev. **136**, B854 (1964).

[20] W. Kohn and L. J. Sham, Phys. Rev. **140**, A1133 (1965).

[21] D. M. Ceperley and B. J. Alder, Phys. Rev. Lett. **45**, 566 (1980).

[22] J. R. Chelikowsky, D. J. Chadi, and M. L. Cohen, Phys. Rev. B **23**, 4013 (1981).

[23] M. Büttiker, Y. Imry, R. Landauer, and S. Pinhas, Phys. Rev. B **31**, 6207 (1985).

[24] N. D. Lang, Phys. Rev. B **45**, 13 599 (1992).

[25] N. D. Lang and W. Kohn, Phys. Rev. B **3**, 1215 (1971).

[26] It is worth noting that the difference of the electron density would contain a phase change similar to the Friedel oscillation. The interpretation of the phase change is not necessarily simple, because the change of the effective potential is caused not only by an applied bias voltage itself but also accompanied charge redistribution. The phase, however, does not seem to affect the bias dependence of the ABH significantly, which is main concern in our research.

[27] R. Wiesendanger, *Scanning Probe Microscopy and Spectroscopy* (Cambridge University Press, Cambridge, 1995), p. 28.

[28] Y. Gohda and S. Watanabe, Phys. Rev. Lett. **87**, 177601 (2001); Surf. Sci. **516**, 265 (2002).